

# Privileged Pooling: Supervised attention-based pooling for compensating dataset bias

Andres C. Rodriguez, Stefano D’Aronco, Jan Dirk Wegner, and Konrad Schindler

EcoVision Lab - Photogrammetry and Remote Sensing, ETH Zurich, Switzerland  
`{firstname.lastname}@geod.baug.ethz.ch`

**Abstract.** In this paper we propose a novel supervised image classification method that overcomes dataset bias and scarcity of training data using privileged information in the form of keypoints annotations. Our main motivation is recognition of animal species for ecological applications like biodiversity modelling, which can be challenging due to long-tailed species distributions due to rare species, and strong dataset biases in repetitive scenes such as in camera traps. To counteract these challenges, we propose a weakly-supervised visual attention mechanism that has access to keypoints highlighting the most important object parts. This privileged information, implemented via a novel privileged pooling operation, is only accessible during training and helps the model to focus on the regions that are most discriminative. We show that the proposed approach uses more efficiently small training datasets, generalizes better and outperforms competing methods in challenging training conditions.

**Keywords:** privileged pooling, weakly-supervised attention, training set bias, fine-grained species recognition, camera trap imagery

## 1 Introduction

Learning under privileged information is a paradigm where, exclusively for the training samples, one has access to supplementary information [27, 40, 20, 19]. The idea is to use this side information to guide the training procedure and achieve a better generalization error. The potential advantages of such an approach are twofold: *(i)* compared to standard supervised learning it is in general possible to achieve better performance with the same (typically small) number of training samples; *(ii)* it is possible to steer the learning so as to overcome potential biases in the training set.

The concept of privileged information during training was originally introduced by [27] to improve the estimation of slack variables and the convergence rate of Support Vector Machines (SVMs). [40, 20, 19] have adapted this idea to a variety of visual tasks, by adding bounding boxes, attributes or sketches as privileged information [26, 6]. Technically, one can interpret privileged information as a way of regularizing the model parameters with additional knowledge about the training samples.

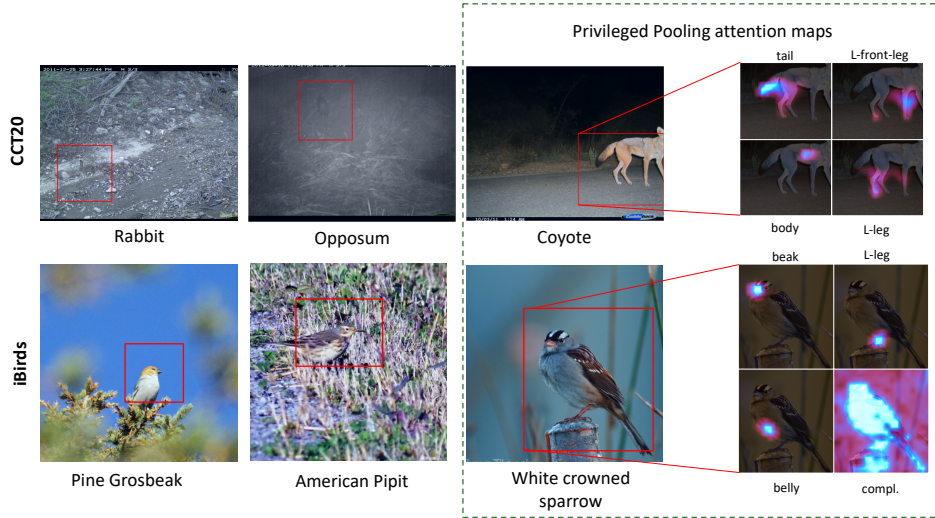


**Fig. 1.** Predicted classes using privileged pooling on CCT20-Cis test dataset (top) and iBirds test dataset (bottom). Bounding boxes are computed using the predicted attention maps. Attention maps (bounding-box cropped for visualization) depict the encode privileged information from different keypoints provided at train time. The bottom right-most attention map is not supervised by any keypoint and acts as complementary to other animal regions.

Many common architectures, like ResNet [11] or Inception [33], employ a global average pooling layer before the final fully connected layer, in order to reduce the number of parameters and to make the model applicable to input images of varying size. However, much information is lost during feature averaging, as features of the object of interest (in our case the animal) are merged with background features. Intuitively, this can lead to noisy representations particularly if the training dataset is small. This can happen in skewed data distributions where some classes appear less frequently than others, as for instance some animal species [36]. A similar problem arises in the scenario of biased sampling that might cause the network to learn spurious correlations irrelevant, or even harmful, for the task [35, 28]. Moreover, global pooling operations harm generalization of the model if categories of interest often appear in the same context, complicating the conceptually simple task to focus on a small relevant region; as for instance in our application where animals are surrounded by similar vegetation. We thus advocate the use of privileged information during training to guide the models’ attention.

We introduce *privileged pooling (PrPool)* a weakly-supervised visual attention mechanism that leverages privileged information in the form of keypoint locations to learn a weighted pooling operation. It is intuitive that annotations of important object parts facilitate learning from small training sets. We use point-wise part annotations, which are relatively cheap to collect and at the same time directly relevant to discriminate objects that look alike (i.e., similar

animal species). Although several studies have looked into self-supervised attention techniques to improve image interpretation tasks [14, 43, 21], our work is, to our knowledge, the first to view attention maps as an encoding of privileged information. We propose an attention gating mechanism that selects relevant features according to the annotated keypoints and pools the feature maps accordingly. The method can be combined with different commonly used pooling schemes to improve classification performance. We also provide a new dataset for this task (Caltech CameraTrap-20+) by augmenting a subset of the Caltech CameraTrap-20 [2] dataset with animal part annotations. Our method significantly improves performance on this challenging dataset by counteracting inherent biases. Furthermore, we test on the CUB200 [37] birds dataset under a scarce data regime, and also outperform prior art based on both privileged information and few-shot learning. To assess generalization, we extract the matching subset of the *aves* (bird) family from the iNaturalist-17 dataset [36], and test the model trained on CUB200. In that experiment the advantage of our model is even bigger. Overall, we show that supervising the pooling with privileged information affords better generalization with fewer training samples, and is also a powerful alternative to few-shot learning when labeled training data is scarce.

## 2 Related work

**Learning under privileged information** attempts to leverage additional information  $\mathbf{x}^*$  during training, but does not rely on it at test time, see Fig. 2. How to best exploit such side information is not obvious. Several algorithms have been developed for SVMs, for tasks including action [26] and image [32] recognition. Applications in the context of deep learning include object detection [13] and face verification [3]. Also simulated data has been interpreted as privileged information [20], and (heteroscedastic) dropout has been used as a way of injecting, at training time, privileged information into the network [19].

**Knowledge Distillation (KD)** [12, 4], originally introduced for model compression, is closely related to the concept of privileged information [24], see Fig. 2. KD trains a student network to imitate the output of (usually much bigger) teacher network pre-trained on the same task. To distil knowledge of both high- and low-level features from a pre-trained teacher, different variants of KD match feature maps at varying stages of the networks, usually to obtain more compact models [29, 15, 41].

**Multitask learning** could be viewed as a naïve way of incorporating privileged side information, by training an auxiliary task to predict the side information, see Fig. 2. The hope is that a shared feature representation will benefit the target task, because it profits from the additional supervision afforded by the auxiliary task. There is a risk that tasks will instead compete for model capacity, leading to decreased performance. Several works focus on the non-trivial task of correctly balancing them [31, 16, 9].

**Few-shot learning** deals with the extension of an already trained classifier to a novel class for which there are only few examples. The hope is that the

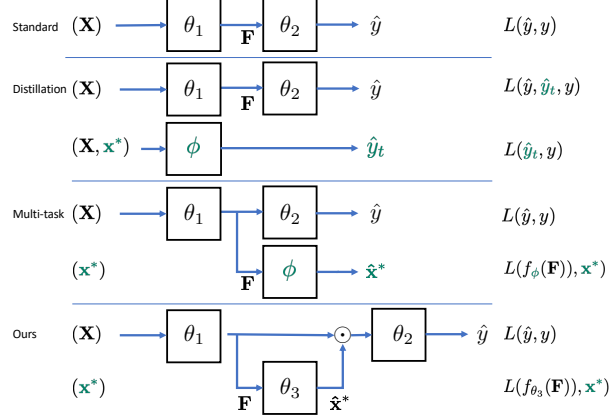


**Fig. 2.** Comparison of learning strategies. In the standard network with parameters  $\theta$ , an input  $\mathbf{x}$  is mapped to a latent encoding  $\mathbf{F}$  and on to a prediction  $\hat{y}$ . Distillation first learns a teacher network with parameters  $\phi$  using also privileged information  $\mathbf{x}^*$ , then learns the weights  $\theta$  to approximate that teacher network. Multi-task learning jointly learns to predict also  $\mathbf{x}^*$  with a decoder with parameters  $\phi$ . The proposed framework adds an attention mechanism with parameters  $\theta_3$  and supervises it with  $\mathbf{x}^*$ . Green denotes quantities used only during training.

new class, when embedded in the previously learned feature space, has a simple distribution that can be learned from few samples [18]. One way to achieve this is to enforce compositionality of the feature space [1, 34] by exploiting additional attributes of the training data, which can be seen as a form of privileged information.

**Pooling.** Virtually all image classification methods use some sort of pooling over a feature map extracted from a feature extractor – nowadays a deep backbone. Beyond simple average- or max-pooling, other methods like bilinear pooling [17, 10], covariance pooling [22, 23] and higher-order estimators [7, 5] have been proposed. These methods are collectively referred to as *second-order methods*, since they estimate second-order statistics of the features distribution. Empirically this can improve discriminative power [23, 7].

Despite recent developments in transfer learning and pooling, it is an open question how to leverage sparse, but highly informative privileged information at train time. We address this with a simple but effective *privileged pooling* scheme.

### 3 Method

Consider a supervised image classification task, with inputs  $\mathbf{X} \in \mathcal{X}$  represented as 3D tensors of size  $w \times h \times c$ , and outputs  $y$  from a label space  $\mathcal{Y}$ . The goal is to learn a function  $f_\theta : \mathcal{X} \rightarrow \mathcal{Y}$  with parameters  $\theta$ , for instance a convolutional

network (CNN), that minimises the expected loss  $l : \mathcal{Y} \times \mathcal{Y} \rightarrow \mathbb{R}$ :

$$\underset{\boldsymbol{\theta}}{\text{minimise}} \quad \mathbb{E}_{p(y, \mathbf{X})} [l(f_{\boldsymbol{\theta}}(\mathbf{X}), y)]. \quad (1)$$

In the paradigm of learning under privileged information, we have access to additional side information denoted by  $\mathbf{x}^* \in \mathcal{X}^*$  for the training examples (but *not* for the test data).  $\mathbf{x}^*$  has size  $d'$ , and is usually of much lower dimensionality than  $\mathbf{X}$  ( $d' \ll whc$ ). We may think of the training set as composed of triplets of the form  $\{\mathbf{X}, \mathbf{x}^*, y\}$ . Because we will only have access to  $\mathbf{X}$  at prediction time, the overall goal is to minimise the risk of Eq. (1). However, we would want to leverage the information afforded by  $\mathbf{x}^*$  to regularise the training procedure. This leads to the a new optimisation problem:

$$\underset{\boldsymbol{\theta}}{\text{minimise}} \quad \mathbb{E}_{p(y, \mathbf{X})} [l(f_{\boldsymbol{\theta}}(\mathbf{X}), y)] + g(\boldsymbol{\theta}, p(\mathbf{X}, \mathbf{x}^*, y)), \quad (2)$$

where  $g$  represents a regulariser that depends on the learned parameters  $\theta$  and on the joint distribution of the triplets  $p(\mathbf{X}, \mathbf{x}^*, y)$ . The challenge is to come up with an appropriate regulariser  $g$  that alters the parameters  $\theta$  such that they reduce the generalisation error for unseen data  $\mathbf{x}$  during test time. For many CNNs,  $f_{\boldsymbol{\theta}}$  can be decomposed into a feature extractor  $f_{\boldsymbol{\theta}_1}(\mathbf{X})$  that yields a feature map  $\mathbf{F}$  of size  $w' \times h' \times c'$ , followed by a (first-order) pooling operation  $\text{pool}(\mathbf{F})$  that yields a feature vector  $\mathbf{p}$  of size  $c'$ , and finally a multi-layer perceptron  $f_{\boldsymbol{\theta}_2}$  that outputs a vector  $\mathbf{y}$  of class scores.

As discussed in Sec. 2, this definition encompasses several forms of transfer learning, e.g., in the case of multi-task learning the second term of the objective function corresponds to  $\mathbb{E}_{p(\mathbf{x}^*, \mathbf{X})} [l(g_{\boldsymbol{\theta}_1}(\mathbf{X}), x^*)]$ , where  $\boldsymbol{\theta}_1$  are the shared parameters of the common feature extractor. This formulation, however, does not guarantee that the main task makes full use of the privileged information prediction. One possible solution to this problem consists in re-feeding the side task prediction in the main network branch. This is exactly the strategy we adopt in our architecture and, since as side information we consider keypoints annotations, we specifically use this privileged information to steer the focus of the main network,  $f_{\boldsymbol{\theta}}$ , towards those locations of the image that are most relevant for solving the main task, in our case animal species classification, i.e., we add a *visual attention* mechanism [39, 25]. To that end we learn attention maps that highlight important locations in the image, see Fig. 3.

### 3.1 Supervision of attention maps

The purpose of attention mechanisms is to emphasize image evidence that supports prediction [30, 21]. In images this is commonly done by means of a  $1 \times 1$  convolution that outputs a weight to re-weight features before passing them to the next layer in a neural network. For example, [14, 43] use attention maps to learn feature gating for fine-grained classification without additional supervision than the image-level class label. Here we explore a weakly supervised attention

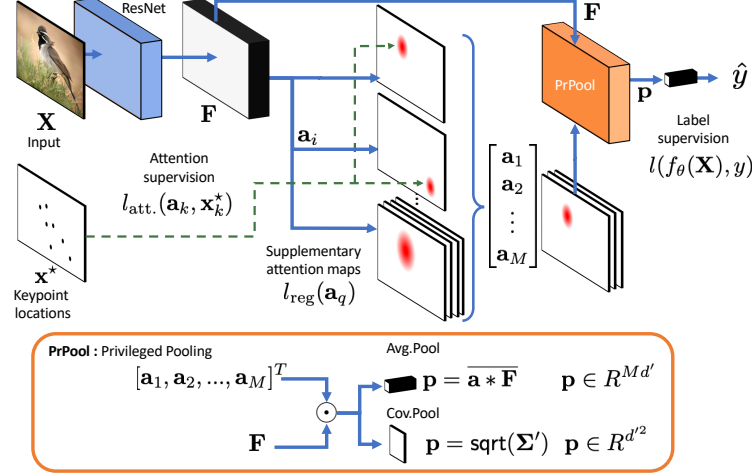


**Fig. 3.** Privileged Pooling (**PrPool**) illustration.  $M$  attention maps with  $K$  supervised and  $Q$  supplementary ones.  $\text{sqrt}(\Sigma)$  is the square-root normalized covariance matrix of attention-weighted re-samples of  $F$ . Green-dotted lines denote quantities used only during training.

mechanism: privileged information in the form of keypoint annotations is available at training time and serves to teach the network how to identify locations of interest in the latent feature representation.

As annotations we provide, for every training image, the desired output label as well as a set of  $K$  keypoint locations. Keypoints are ordered and every point has a fixed semantic meaning, in our case a specific body part of the animal. We found that scheme particularly effective for our application, as it delivers highly informative privileged information with fairly low annotation effort.

Our proposed privileged information framework is depicted in Fig. 2. We add a network branch that derives  $K$  attention maps  $\mathbf{a}_k$  from the feature map  $\mathbf{F}$ . In contrast to previous approaches we rely on  $3 \times 3$  convolutions to produce the attention maps. This is necessary since we need to have a larger receptive field to produce attention maps that re-weight based on higher level concepts from the image (i.e. head, tail, etc.) instead of just the feature vector it self.

Each map has size  $w' \times h'$  and takes on continuous values in the interval  $[0, 1]$ . The extraction of the attention maps is supervised with a binary cross-entropy loss w.r.t. the keypoint annotations  $\mathbf{x}^*$ ,

$$l_{\text{BCE}}(\mathbf{a}_k, \mathbf{x}_k^*) = \frac{1}{W'H'} \sum_{w,h} x_{whk}^* \log(a_{whk}) + (1 - x_{whk}^*) \log(1 - a_{whk}). \quad (3)$$

Because the keypoint annotation might sometimes not be exactly at the right position, it is convenient to adopt a multi-scale loss. Attention map and keypoint map are passed through a resizing operator  $s \in [s_1..s_J]$  and the losses (Eq. 3)

computed at different resolutions are combined:

$$l_{\text{attention}}(\mathbf{a}_k, \mathbf{x}_k^*) = \sum_j l_{\text{BCE}}(s_j(\mathbf{a}_k), s_j(\mathbf{x}_k^*)) \quad (4)$$

This multi-scale attention loss  $l_{\text{attention}}$  (Eq. 4) is then applied separately to all  $K$  keypoint maps.

Additionally, we include supplementary attention maps whose supervision comes only from the main classification loss. This allows the network to attend other potentially important regions not indicated by keypoints. It is however not trivial how to use them since without additional supervision the optimization might converge to the trivial solution of an uniform map, or having all attention maps attending the same areas. Center loss [38] has been successfully used for enforcing a single feature center per label and penalize distances from deep features to their corresponding center, see [14]. We empirically found that, in our case, a much simpler regularization that maximizes the variance within each attention map yields better results:

$$\bar{\mathbf{a}}_i = \frac{\sum_{w', h'} \mathbf{a}_i}{w' h'} \quad l_{\text{reg}}(\mathbf{a}_i) = \bar{\mathbf{a}}_i * (1 - \bar{\mathbf{a}}_i) \quad (5)$$

To understand that regulariser, note that it imposes a bias against trivial maps that are overly diffuse (or, in the extreme case, uniform). See Figure 3 for an overview of the complete method. The final loss for a model with  $K$  supervised and  $Q$  supplementary attention maps is defined as:

$$L = l(f_{\theta}(\mathbf{X}), y) + \frac{1}{K} \sum_k l_{\text{attention}}(\mathbf{a}_k, \mathbf{x}_k^*) + \frac{1}{Q} \sum_q l_{\text{reg}}(\mathbf{a}_q) \quad (6)$$

### 3.2 Attention pooling

The attention maps are used to pool the feature map  $\mathbf{F}$  multiple times to obtain the vector  $\mathbf{p}$ . Different pooling schemes can be employed.

*First Order Pooling* comprises average and max pooling, the most common pooling operations. [42] demonstrate that combining average and max pooling operations yields to better results on the CUB dataset for fine-grained classification. Similar to [14], we use each of the attention maps to perform a pooling operation of the feature map with different weightings  $\text{pool}(\mathbf{a}_i * \mathbf{F})$ . Pooling individually for each attention map means that the regions highlighted by them are emphasized, and some degree of locality is preserved. The features of different maps are simply concatenated.

*Second Order Pooling* regards each pixel in the feature map as a sample and computes a covariance matrix of all the features. The feature map  $\mathbf{F}$  is reshaped

to  $c' \times s$ , where  $s$  is the number of pixels in map  $\mathbf{F}$  of size  $w' \times h'$ . The covariance matrix with  $s$  samples is:

$$\mathbf{\Sigma} = \frac{1}{s}(\mathbf{F} - \bar{\mathbf{F}})(\mathbf{F} - \bar{\mathbf{F}})^T \quad (7)$$

Furthermore, [23] showed that normalising  $\mathbf{\Sigma}$  by taking its square root, denoted here as  $\text{sqrt}(\mathbf{\Sigma})$ , drastically improves the representation power of the features. Computing the square root of the covariance matrix is however not a simple task. Some methods rely on SVD decomposition, such as [23], a better method consists in using the Newton-Schulz iterative matrix square root computation which can be implemented more efficiently on GPU [22].

In order to use the covariance pooling method similarly to [22], we propose to compute the Hadamard product of each attention map with  $\mathbf{F}$  to obtain  $\mathbf{F}'$ , an attention-weighted feature map. In this way, we can improve the robustness of the  $\text{sqrt}(\mathbf{\Sigma})$  computation when a limited amount of labeled training samples are available. Now, we can reshape  $\mathbf{F}'$  to a matrix of size  $d \times as$ , where  $a$  is the number of attention maps. We observed that treating product  $\mathbf{a}_i * \mathbf{F}$  as a new set of  $s$  samples yielded better empirical results; it intuitively gives more freedom to the network to attend pixels more than once in different contexts (i.e., pooling the same pixel weighted differently, due to different attention maps might be beneficial). Finally, note that since the complete operation can be back-propagated, the network tunes the attention maps that would give the best features to compute the covariance matrix.

## 4 Experiments

We now evaluate the proposed method on two different datasets, show how it improves over Average Pooling and Covariance Pooling; and compare its performance against other methods that also leverage privileged information.

### 4.1 Datasets

**CUB200** [37] is a dataset of 200 different bird species, with a total of 5994 training images and 5794 test images. Each image comes with 15 keypoint annotations for body parts such as beak, belly, wings, etc. CUB200 has been extensively used for fine-grained image classification and highly specialised architectures have been designed for it. Still, a vanilla ResNet-50 pretrained on ImageNet achieves 86% accuracy (note that ImageNet includes some bird classes, and there might even be some common images between the two datasets).

Our focus is to evaluate keypoint annotations as privileged information to (i) train a model in data-scarce settings, and (ii) improve the generalization to other data. Images in CUB200 are usually centered on the bird and depicted in “standard” poses suitable for recognition, as in a field guide. To test generalization, we use images from the iNaturalist-2017 [36] dataset, which features less curated, more challenging images of birds. 156 birds species are shared between



CUB200 and iNaturalist-2017, for those species there are in total 3407 images (average 22 samples/species) in iNaturalist-2017, which we use as an additional test set, termed **iBirds**.

**Caltech CameraTrap-20+ (CCT20+)** is a reduced version of CCT20[2] augmented with privileged information. CCT20 is a set of 57,000 images captured at 20 different camera locations and showing 15 different animal classes.<sup>1</sup> Images from 10 camera locations and taken on even days form the training set (13k samples). There are two different test scenarios. The “Cis” split (15k samples) consists of the odd days of the same cameras used for training, to test generalization across time for a fixed set of viewpoints. The “Trans” split (23k samples) are images from camera locations not seen during training, to test generalization to new viewpoints. As validation data, a single day (3.4k samples) for the Cis scenario, respectively a single location (3.4k samples) for the Trans scenario, is held out from the training data.

*CCT20+* augments CCT20 with privileged information that we manually annotated for 1182 images across all species and all cameras of the training set. We chose keypoints that have the same semantic meaning across the different species of animals in the dataset: head, left-front-leg, right-front-leg, left-back-leg, right-back-leg, tail and body-center. One day of student work was required to write and use a small python script for keypoint annotation.

In our experiments we do not use the sequence information but treat every image independently. Moreover, we disregard images with more than one animal species and images without any annotated bounding box (the bounding box is not used in our system, we only use it as an indication that an animal was visible for the human annotator). See the supplementary material for further details about the dataset.

## 4.2 Implementation Details

All experiments have been implemented in Pytorch, with Resnet-101 pre-trained on ImageNet as backbone. *WS-DAN* was implemented in Tensorflow and uses InceptionV3 as a backbone. For experiments with Covariance Pooling we used the pretrained Resnet-101 from [22]. For all comparisons, we included open-source code from the respective authors into our pipeline. Data augmentation is standardized across all models: images are resized with a random scale in  $[0.5, 1]$  and random cropping to  $488 \times 488$  pixels. Test images are resized to  $448^2$  pixels for CUB and  $600^2$  pixels for CCT. All our models are trained with SGD with momentum 0.9 and weight-decay  $10^{-4}$ , batch-size 10 and initial learning-rate of 0.01, a backbone multiplier of 0.01, and exponential decay by a factor 0.9 every 1000 iterations. Finally, some methods, such as [14], leverage the predicted attention maps at inference time to crop the image around the most important parts and re-feed it through then network. The final prediction is obtained by averaging the two single prediction. This a general strategy is orthogonal to

<sup>1</sup> CCT20 is a subset of the bigger Caltech CameraTrap set with 243k images from 140 locations.

what we propose in this paper, and can be applied to any method that predicts attention maps. For a fair comparison we apply re-feeding to all the methods that allow this operation; in the supplementary we provide the results obtained without re-feeding.

### 4.3 Baselines

**No- $x^*$  Methods** *AvgPool*: is a vanilla Resnet-101 pre-trained on ImageNet, with average pooling and a single fully connected layer for final prediction.

*WS-DAN Avg* [14] is a method that reaches state-of-the-art results on several fine-grained image classification datasets including CUB200, FGVC-Aircraft, Stanford Cars and Stanford Dogs. It uses unsupervised learning of attention maps to perform weighted pooling.

iSQRT [22] (*CovPool*) proposes to change the usual average pooling of feature maps with a square-root normalized covariance pooling. Empirically this is particularly useful for fine-grained classification, where 2<sup>nd</sup>-order information can be highly informative.

S3N [8] proposes a way to select peaks of the feature response, so as to force the network to explore those peaks, which can be especially informative for the prediction. That method also achieves state-of-the-art performance on CUB200, but it does so at a high cost:  $c'^2$  additional parameters are required for the peak sampling layers from a feature map of size  $w' \times h' \times c'$ .

**$x^*$  Methods** We test our method *PrPool* in combination with both average and covariance pooling. *PrPoolN* denotes  $N$  additional unsupervised attention maps. According to the keypoint numbers, there are 15 supervised attention maps for CUB200 and 7 for CCT20, unless noted otherwise.

The *multitask* architecture is identical to *AvgPool*, except that the output of the backbone is also connected to a fully connected layer that predicts the keypoints locations. This baseline represents a sort of "lower bound" for the impact of privileged information that is available only during training.

*SimGrad* [9] is an improvement of the multitask architecture that aims at reducing the risk that the auxiliary task harms the main task. After separately computing the gradients of the two tasks w.r.t. the shared parameters, the gradients are averaged only if the cosine similarity between them is positive. Otherwise the auxiliary loss is ignored, with the intuition that it should not influence the fitting if it is in conflict with the primary loss.

For knowledge distillation (*KD*) we train a classification network that has two input channels, one for the RGB images and one for the keypoint masks. Once trained, we distill the output of that teacher network into our baseline Resnet101 as student model.

Heteroscedastic dropout (*h-dropout*) [19] highlights how learning under privileged information can be implemented via a dropout regularization. We tried to implement that method in conjunction with other attention-based methods

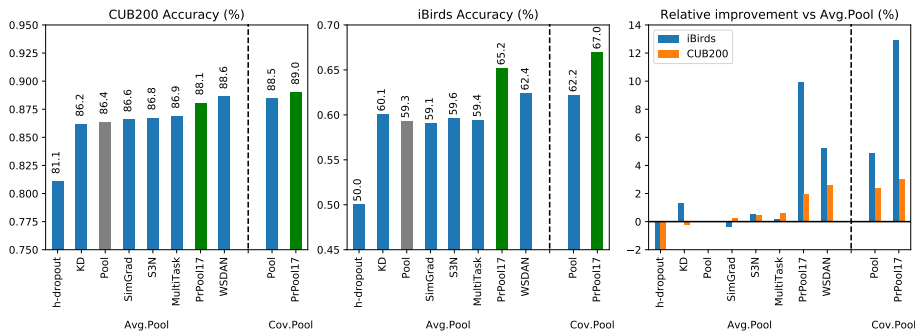


**Fig. 4.** top-1 accuracy for CUB (left) and iBirds (middle) test datasets. in gray the baseline method *PoolAvg*, and green indicates our methods trained with *PrPool*. Left: Relative improvement vs the baseline method. Methods marked with + use attention cropping at test time.

(e.g., [14]), but found that despite our best effort the noise injected into the fully connected layer made training of the attention maps unstable.

A main goal of our work is to learn classes for which we only have few training examples, so it is also related to few-shot learning. We test compositional *FewShot* recognition [34], which uses class-level labels to enforce compositionality (see Sec. 2). We use the same 5 random splits into base classes and novel classes as [34] and run our *PrPool* network on them, uniformly sampling from the batches when creating a batch, in order to deal with the imbalance between novel and base classes.

#### 4.4 Fine-grained classification

Figure 4 presents the results on the CUB200 test set. The average pooling baseline (*AvgPool*) achieves 86.4%. With average pooling supervised by privileged information (*PrPool*), this increases to 87.7%. In line with the literature [22] we find that covariance pooling is superior to average pooling for fine-grained-classification, reaching 88.5%. But again, privileged pooling improves the result further to 89.0%. These improvements may seem comparatively small. When, however, testing the trained networks on iBirds, the gains are amplified, i.e., our models with supervised attention generalise better. The relative improvements are quite significant, up to 9.2% over the average pooling baseline (Fig. 4, right). While most baselines show a mild improvement over the baseline on CUB200, but do not reach the performance of *PrPool*; we find that they even fall behind the baseline in iBirds, seemingly they are to some degree overfitted to the CUB200 distribution and not able to generalise.

Samples per class		iBirds			CUB		
		5	10	15	5	10	15
Avg	MultiTask	33.6	47.2	52.5	61.7	77.5	81.5
	Pool	39.3	49.1	54.6	66.0	77.9	81.7
	PrPool17	48.5	58.1	60.3	73.8	82.5	84.6
	S3N	38.8	49.6	54.0	67.2	79.6	82.4
	SimGrad	34.6	47.4	53.2	62.7	77.7	81.8
	WSDAN	38.5	51.8	56.0	68.8	80.4	84.1
Cov	Pool	45.5	56.2	58.8	72.0	82.4	85.0
	PrPool17	<b>49.6</b>	<b>59.6</b>	<b>62.8</b>	<b>74.6</b>	<b>83.3</b>	<b>85.4</b>

**Table 1.** Top1 Accuracy for CUB200 and iBirds test set. Best performance in **bold**.

#### 4.5 Data Efficiency

Privileged information especially improves the data efficiency in data-scarce regimes. To simulate smaller training sets, we draw  $n$  samples per class out of the training data. Table 1 shows that *PrPool* consistently outperforms all competing approaches, with increasing benefits as the training set gets smaller. Note that in the most challenging 5-shot case, there are only 1000 samples to learn 200 classes. We also find that in the small data regime, the naïve multi-task loss does not improve performance, and also other baselines become rather inconsistent.

*Comparison to Few-shot Learning* Given the performance achieved with only 5 samples per class, we also compare to few-shot learning. We use the same evaluation strategy of [34] using 100 base classes and 100 new classes with only  $n$  shots each, results can be seen in Figure 5. As expected, dedicated few-shot learning based on a set of well-trained base classes and some form of distance learning to add the new classes is superior in the extreme 1-shot and 2-shot scenario. But already in the 5-shot case, we find that even simple average pooling is competitive with few-shot learning, and our privileged pooling already outperforms it. At 10 samples the difference is accentuated, as one moves further away from the extreme few-shot setting. Apparently the privileged information can, already at this low sample number, compensate the reduced sampling of the pose and appearance space, by steering the learning towards sub-regions with a well-defined semantic meaning across classes.

As before we evaluate the implemented methods on the iBirds dataset, see Figure 5. Results are consistent with the previous ones, *PrPool* proves to be very effective at increasing performance in low-data regime and improves the generalization power of the network.

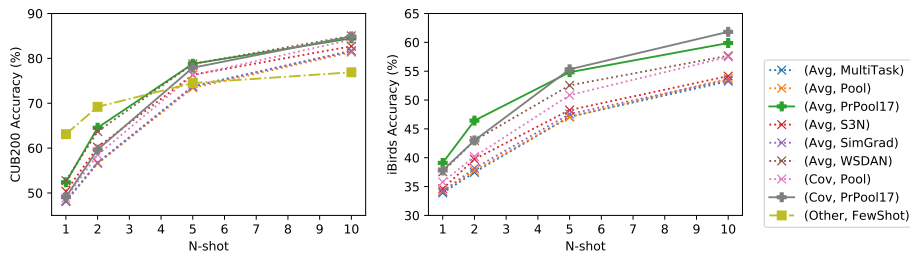


**Fig. 5.** CUB200 (left) and iBirds (right) Top1 Accuracy. 100 base classes, with 100-way new classes with  $n$ -shots. Average over five random novel/base splits. Methods with  $+$  marker denote PrPool (ours). FewShot results from [34]

#### 4.6 Generalization with biased datasets

Figure 6 and Table 4.6 show the results on CCT20. That dataset is very challenging, due to bad illumination, frequent occlusions, camouflage and extreme perspective that arise in camera traps. Moreover, the highly repetitive scenes are an “invitation to overfit” and learn spurious correlations, which then hinder generalization to new scenarios (e.g., unseen camera locations). Our *PrPool* method achieves the best performance. In this case, with fewer and more distinct classes, first-order pooling works better than *CovPool* (but also the latter outperforms the baselines).

Note that our method trained only on the CCT20+ subset with  $\approx 1000$  samples outperforms the *AvgPool* baseline even when the latter is trained with  $10\times$  more samples. We see two reasons for this, (i) the superior data efficiency through Privileged Pooling, and (ii) the low diversity of samples in Camera Trap data, where more samples can in fact reinforce inherent dataset biases. In the most challenging Trans-location setting *PrPool* reaches 72% test set accuracy.

#### 4.7 Ablation study: supervision of attention maps

We go on to analyze how important attention map supervision is in our architecture, in combination with both average and covariance pooling. To that end we train exactly the same architecture as *PrPool*, but without the supervision signal  $l_{\text{msa}}$  from keypoint annotations. The results in Table 4.7 confirm that the privileged information plays an important role and significantly increases prediction performance. Moreover, we observe that already the regulariser alone improves over totally unconstrained self-attention, as expected.

## 5 Conclusions

The aim of learning under privileged information is to exploit collateral information that is available only for the training data, so as to learn predictors that generalize better. We have examined the case where the privileged information

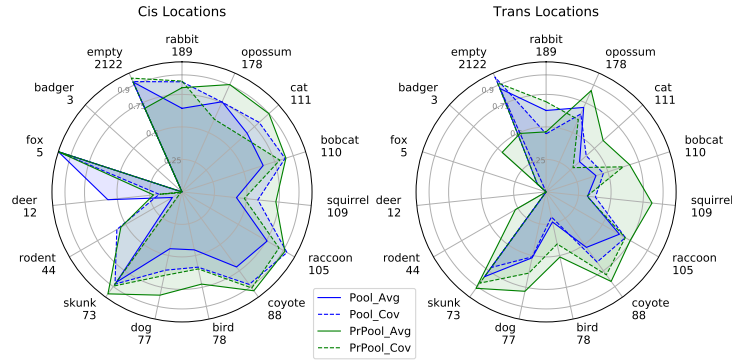


**Fig. 6.** Accuracy per class in CCT20 test datasets. Total training samples 13k including CCT20+ 1180 samples with keypoint annotation and 2122 empty class samples. Numbers below animal classes indicate training samples with keypoints per class. Methods with PrPool (ours) marked in green. Solid lines denote avg-pooling, dashed lines cov-pooling.

comes in the form of keypoint locations, a natural and fairly frequent situation in image analysis. By using keypoints as supervision for attention maps, they can be effectively leveraged to support image classification. Privileged information to steer a model’s attention is particularly effective when labeled training data is scarce, and when it exhibits strong biases. Moreover, it turns out that in some small-data scenarios a moderate amount of privileged information may serve as an alternative to few-shot learning.

On a more general note, we see it as an important message of our work that gathering more data is not the only option to fix an under-trained deep learning model. While additional training data is almost always welcome, there are important applications where it is inherently hard to come by. It is encouraging that, with the right design, more elaborate labeling of the existing data can also present a way forward.

		Cis Locations				Trans Locations			
		Acc		Acc <sub>class</sub>		Acc		Acc <sub>class</sub>	
Training		1k	13k	1k	13k	1k	13k	1k	13k
Avg	MultiTask	72.2	76.4	59.5	65.8	65.6	67.2	42.6	50.0
	Pool	71.4	73.6	57.0	59.8	65.1	66.1	42.0	43.6
	PrPool	<b>80.3</b>	<b>82.1</b>	<b>66.8</b>	<b>73.3</b>	<b>72.0</b>	68.5	<b>55.1</b>	<b>60.2</b>
	S3N	75.2	75.5	61.7	66.7	64.2	<b>70.6</b>	40.2	50.9
	WSDAN	71.7	75.7	50.8	64.9	60.3	62.5	33.5	42.5
Cov	Pool	74.3	81.4	59.8	69.3	67.2	70.1	41.9	43.8
	PrPool	68.8	75.9	46.7	56.3	64.8	70.5	41.2	49.5

**Table 2.** Overall accuracy and mean per class accuracy results of models trained on CCT20 (13k samples), respectively CCT20+ (1k samples with keypoint annotations). Best performance in **bold**.

Supervision Type	iBirds			CUB		
	No	Reg	Pr	No	Reg	Pr
Avg Pool	60.3	61.7	65.2	84.3	87.0	88.1
Cov Pool	62.3	66.5	67.0	87.1	88.5	89.0

**Table 3.** Top1 Accuracy results of attention maps with different supervisions: **P**rivileged supervision ( $l_{\text{attention}}(\mathbf{a}_k, \mathbf{x}_k^*)$ ), **N**o supervision and **R**egularized supervision ( $l_{\text{reg}}(\mathbf{a}_q)$ )

## References

1. Andreas, J.: Measuring compositionality in representation learning. In: ICLR (2019)
2. Beery, S., Van Horn, G., Perona, P.: Recognition in terra incognita. In: ECCV (2018)
3. Borghi, G., Pini, S., Grazioli, F., Vezzani, R., Cucchiara, R.: Face verification from depth using privileged information. In: BMVC (2018)
4. Buciluă, C., Caruana, R., Niculescu-Mizil, A.: Model compression. In: ACM SIGKDD (2006)
5. Cai, S., Zuo, W., Zhang, L.: Higher-order integration of hierarchical convolutional activations for fine-grained visual categorization. In: ICCV (2017)
6. Chen, Y., Jin, X., Feng, J., Yan, S.: Training group orthogonal neural networks with privileged information. In: IJCAI. pp. 1532–1538. AAAI Press (2017)
7. Cui, Y., Zhou, F., Wang, J., Liu, X., Lin, Y., Belongie, S.: Kernel pooling for convolutional neural networks. In: CVPR (2017)
8. Ding, Y., Zhou, Y., Zhu, Y., Ye, Q., Jiao, J.: Selective sparse sampling for fine-grained image recognition. In: ICCV. pp. 6599–6608 (2019)
9. Du, Y., Czarnecki, W.M., Jayakumar, S.M., Pascanu, R., Lakshminarayanan, B.: Adapting auxiliary losses using gradient similarity. arXiv preprint arXiv:1812.02224 (2018)
10. Gao, Y., Beijbom, O., Zhang, N., Darrell, T.: Compact bilinear pooling. In: CVPR (2016)
11. He, K., Zhang, X., Ren, S., Sun, J.: Deep residual learning for image recognition. In: CVPR (2016)
12. Hinton, G., Vinyals, O., Dean, J.: Distilling the knowledge in a neural network. arXiv preprint arXiv:1503.02531 (2015)
13. Hoffman, J., Gupta, S., Darrell, T.: Learning with side information through modality hallucination. In: CVPR (2016)
14. Hu, T., Qi, H.: See better before looking closer: Weakly supervised data augmentation network for fine-grained visual classification. arXiv preprint arXiv:1901.09891 (2019)
15. Jang, Y., Lee, H., Hwang, S.J., Shin, J.: Learning what and where to transfer. arXiv preprint arXiv:1905.05901 (2019)
16. Kendall, A., Gal, Y., Cipolla, R.: Multi-task learning using uncertainty to weigh losses for scene geometry and semantics. In: CVPR (2018)
17. Kim, J.H., On, K.W., Lim, W., Kim, J., Ha, J.W., Zhang, B.T.: Hadamard product for low-rank bilinear pooling. arXiv preprint arXiv:1610.04325 (2016)
18. Lake, B.M., Salakhutdinov, R., Tenenbaum, J.B.: Human-level concept learning through probabilistic program induction. *Science* **350**(6266), 1332–1338 (2015)
19. Lambert, J., Sener, O., Savarese, S.: Deep learning under privileged information using heteroscedastic dropout. In: CVPR (2018)
20. Lee, K.H., Ros, G., Li, J., Gaidon, A.: SPIGAN: Privileged adversarial learning from simulation. In: ICLR (2019)
21. Li, K., Wu, Z., Peng, K., Ernst, J., Fu, Y.: Tell me where to look: Guided attention inference network. In: CVPR (2018)
22. Li, P., Xie, J., Wang, Q., Gao, Z.: Towards faster training of global covariance pooling networks by iterative matrix square root normalization. In: CVPR (2018)
23. Li, P., Xie, J., Wang, Q., Zuo, W.: Is second-order information helpful for large-scale visual recognition? In: ICCV (2017)



24. Lopez-Paz, D., Schölkopf, B., Bottou, L., Vapnik, V.: Unifying distillation and privileged information. In: ICLR (2016)
25. Lu, J., Xiong, C., Parikh, D., Socher, R.: Knowing when to look: Adaptive attention via a visual sentinel for image captioning. In: The IEEE Conference on Computer Vision and Pattern Recognition (CVPR) (July 2017)
26. Motiian, S., Piccirilli, M., Adjeroh, D.A., Doretto, G.: Information bottleneck learning using privileged information for visual recognition. In: CVPR (2016)
27. Pechyony, D., Vapnik, V.: On the theory of learning with privileged information. In: NeurIPS (2010)
28. Ritter, S., Barrett, D.G., Santoro, A., Botvinick, M.M.: Cognitive psychology for deep neural networks: A shape bias case study. In: ICML (2017)
29. Romero, A., Ballas, N., Kahou, S.E., Chassang, A., Gatta, C., Bengio, Y.: Fitnets: Hints for thin deep nets. arXiv preprint arXiv:1412.6550 (2014)
30. Selvaraju, R.R., Cogswell, M., Das, A., Vedantam, R., Parikh, D., Batra, D.: Grad-cam: Visual explanations from deep networks via gradient-based localization. In: ICCV (2017)
31. Sener, O., Koltun, V.: Multi-task learning as multi-objective optimization. In: NeurIPS (2018)
32. Sharmanska, V., Quadrianto, N., Lampert, C.H.: Learning to rank using privileged information. In: ICCV (2013)
33. Szegedy, C., Liu, W., Jia, Y., Sermanet, P., Reed, S., Anguelov, D., Erhan, D., Vanhoucke, V., Rabinovich, A.: Going deeper with convolutions. In: CVPR (2015)
34. Tokmakov, P., Wang, Y.X., Hebert, M.: Learning compositional representations for few-shot recognition. In: ICCV (2019)
35. Torralba, A., Efros, A.A.: Unbiased look at dataset bias. In: CVPR (2011)
36. Van Horn, G., Mac Aodha, O., Song, Y., Cui, Y., Sun, C., Shepard, A., Adam, H., Perona, P., Belongie, S.: The iNaturalist species classification and detection dataset. In: CVPR (2018)
37. Welinder, P., Branson, S., Mita, T., Wah, C., Schroff, F., Belongie, S., Perona, P.: Caltech-UCSD Birds 200. Tech. Rep. CNS-TR-2010-001, California Institute of Technology (2010)
38. Wen, Y., Zhang, K., Li, Z., Qiao, Y.: A discriminative feature learning approach for deep face recognition. In: ECCV (2016)
39. Xu, K., Ba, J., Kiros, R., Cho, K., Courville, A., Salakhudinov, R., Zemel, R., Bengio, Y.: Show, attend and tell: Neural image caption generation with visual attention. In: International conference on machine learning. pp. 2048–2057 (2015)
40. Yang, H., Tianyi Zhou, J., Cai, J., Soon Ong, Y.: Mimpl-fcn+: Multi-instance multi-label learning via fully convolutional networks with privileged information. In: CVPR (2017)
41. Zagoruyko, S., Komodakis, N.: Paying more attention to attention: Improving the performance of convolutional neural networks via attention transfer. In: ICLR (2017)
42. Zhang, L., Huang, S., Liu, W., Tao, D.: Learning a mixture of granularity-specific experts for fine-grained categorization. In: ICCV (2019)
43. Zheng, H., Fu, J., Mei, T., Luo, J.: Learning multi-attention convolutional neural network for fine-grained image recognition. In: ICCV (2017)

## 6 Supplementary Material

### 6.1 Analysis of attention cropping at test time

Using the attention maps from *WSDAN* and *PrPool*(ours) it is straight forward to create a bounding box around the areas in the image that the network is attending to. We used this bounding box to crop the image and re-feed it at test time. We observed this is a key element of *WSDAN* and has a positive effect in most of the cases. However, it decreases the performance on CUB for Covariance *PrPool*. See Table 4. In general, this intuitively increases performance as it creates a higher-resolution attention map from the cropped input image (The original image is of size  $488^2$  and the attention map is  $28^2$ ).

The results for the CCT20 dataset can be seen in Table 5, the effect of the re-feeding is not clear in this case. For Cis locations it seems that re-feeding actually hurts model performance. As in some images the animals appear extremely small in this dataset, we speculate the performance drop might be possibly caused by some undesired artifacts that occur at high upsampling factors.

### 6.2 CCT Dataset details

See Table 6 for some details regarding the composition of the train, train+ (annotated samples with keypoints), validation and test sets for the CCT20 dataset. As mentioned in the experiments, we discard the sequence information and images with multiple animal species.

### 6.3 CCT Results with only CCT+ as train dataset

We now explore the impact that privileged information has when using only the keypoint annotated images from CCT20+ dataset. As expected, the differences in performance with respect to the baseline methods are larger in this case. See Figure 7 for more details on the per class performance.

### 6.4 Example attention maps of trained models

See Figure 8 for random samples of predictions and attention maps over the Cis Test. In this samples, we observe that the attention maps clearly highlight the different keypoints, even when the animal is difficult to distinguish with respect to the background. Figure 9 on the other hand, shows samples from the iBirds test dataset. Here the bottom right attention map is supplementary to the keypoints and effectively performs a fore-ground back-ground separation.

Model	Test-crop	iBirds	CUB
Avg PrPool17	No	61.4	87.7
	Yes	<u>65.2</u>	<u>88.1</u>
WSDAN	No	54.9	87.4
	Yes	<u>62.4</u>	<u>88.6</u>
Cov PrPool17	No	64.8	<b>89.4</b>
	Yes	<b>67.0</b>	89.0

**Table 4.** CUB200 and iBirds Test datasets results. Effect of re-feeding attention-cropped images at test time with *WSDAN* and *PrPool* models. Best performance for each case is underlined. In **Bold** the best overall performance.

		Cis Locations				Trans Locations			
		Acc		Acc <sub>class</sub>		Acc		Acc <sub>class</sub>	
	Training	1k	13k	1k	13k	1k	13k	1k	13k
Pool Model	Test-crop								
Avg PrPool	No	<b>81.0</b>	<b>83.5</b>	<b>69.4</b>	70.3	70.6	<u>72.3</u>	52.7	54.8
	Yes	80.3	82.1	66.8	<b>73.3</b>	<b>72.0</b>	68.5	<b>55.1</b>	<b>60.2</b>
	WSDAN	No	<u>72.9</u>	<u>76.2</u>	<u>52.2</u>	63.9	<u>62.6</u>	61.4	<u>34.7</u>
		Yes	71.7	75.7	50.8	<u>64.9</u>	60.3	<u>62.5</u>	<u>42.5</u>
Cov PrPool	No	<u>76.7</u>	<u>82.9</u>	<u>57.0</u>	<u>69.9</u>	<u>68.5</u>	<b>75.0</b>	<u>42.8</u>	<u>51.6</u>
	Yes	68.8	75.9	46.7	56.3	64.8	70.5	41.2	49.5

**Table 5.** CCT20 Test datasets results. Effect of re-feeding attention-cropped images at test time with *WSDAN* and *PrPool* models. Best performance for each model with or without test-cropping is underlined. In **Bold** the best overall performance.

Class	Datasplit					
	Train	Train+	Val		Test	
			Cis	Trans	Cis	Trans
All	13,139	1,182	3,408	1,605	15,469	22,626
opossum	2,470	178	346	425	3,988	4,614
rabbit	2,190	189	320	9	1,461	669
empty	2,122	0	1,860	192	3,922	6,355
coyote	1,200	88	161	43	1,096	1,706
cat	1,164	111	169	70	1,455	1,233
squirrel	1,024	109	146	0	496	779
raccoon	845	105	116	108	869	4,314
bobcat	673	110	92	624	751	1,901
dog	580	77	89	80	627	631
bird	353	78	36	5	360	127
rodent	260	44	46	0	140	22
skunk	212	73	24	49	162	263
deer	38	12	2	0	136	0
fox	5	5	0	0	2	1
badger	3	3	1	0	4	11

**Table 6.** Samples per class in the CCT20 and CCT20+ (marked as Train+) dataset after disregarding cars class and sequence information.

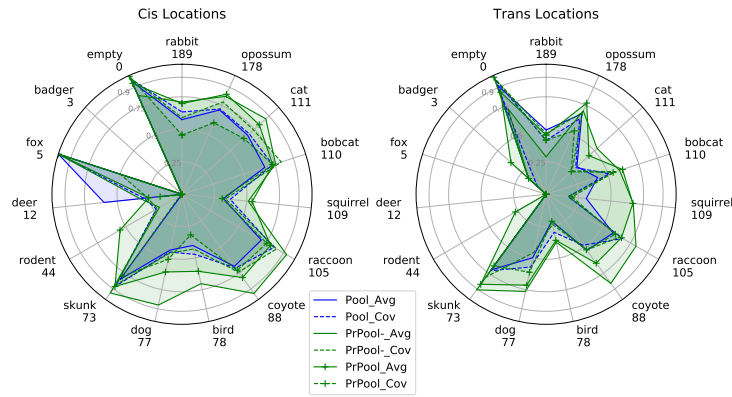


**Fig. 7.** Accuracy per class in CCT20 dataset. Training only 1,180 with keypoint annotation). Methods with PrPool (ours) marked as **Green**. Average Pooling with solid-line and Cov. Pooling with dotted-line. Methods with (–) denote no test-cropping.

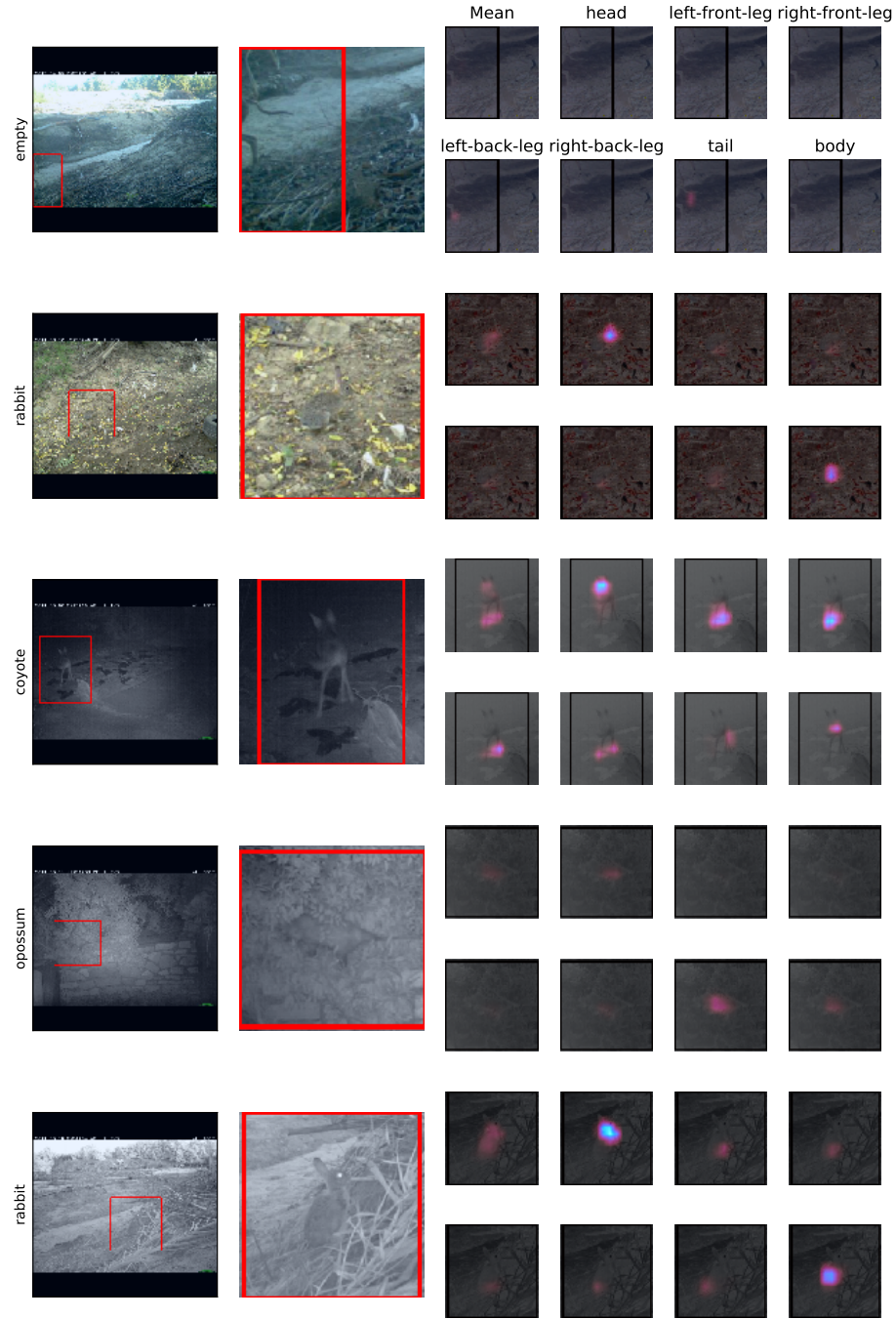


**Fig. 8.** Random samples from CCT Cis Test set. Bounding Box in red is derived from the supervised attention maps. Input image in first column (with predicted class in y axis), zoom to attended region in second column. Keypoint specific attention maps.

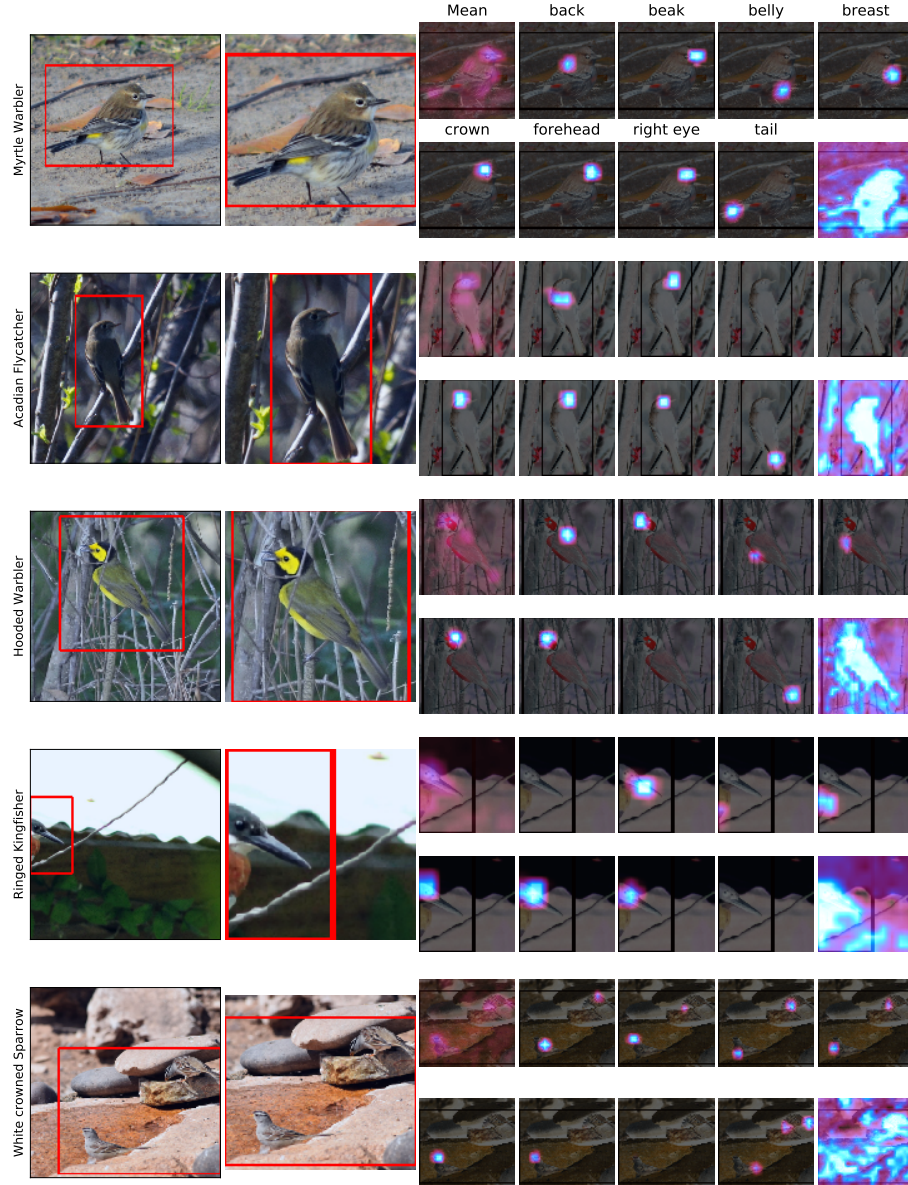


**Fig. 9.** Random samples from iBirds Test set. Bounding Box in red is derived from the supervised attention maps. Input image in first column (with predicted class in y axis), zoom to attended region in second column. Keypoint specific attention maps.